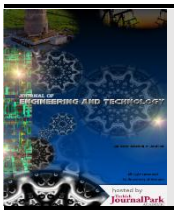

Journal of Engineering and Technology
DergiPark
AKADEMİK

Journal of Engineering and Technology

The Hydrothermal Synthesis of ZnO-CdO Composite and Physical and Electrical Characterization

Canan Aksu Canbay*[1], Safiye Jameel Biro[1], İskender Özkul[2]

[1]Firat University, Department of Physic. Elazig, TURKEY

[2]Mersin University, Department of Mechanical Engineering, Campus, Yenisehir, Mersin, TURKEY

ARTICLE INFO

Article history:
Received 30 Nov 2018
Received in revised form 26 Dec 2018
Accepted 27 Dec 2018
Available online 28 Dec 2018

Key words:
Zinc oxide,
hydrothermal method,
optical band gap,
TG-DTA.

* Corresponding author.
E-mail address: Caksu@firat.edu.tr

ABSTRACT

In this study, ZnO-CdO composites were synthesized by hydrothermal method. Two different contents of the nano-composites have been fabricated for the investigation of structural, morphological, optical and electrical properties. X-ray diffraction (XRD), FTIR, scanning electron microscopy (SEM), UV-VIS-NIR spectrophotometer and two probe methods were used for these analyses. At the same time, the chemical analysis of the sample was measured by EDX analysis. The TG-DTA analyses were made to determine the thermal stability. The optical band gap of composites was found to be 2.78 and 3.06 eV, respectively, with an increase in the content of the Zn precursor.

1. Introduction

Today, the development of nanotechnology has affected all areas of the industry, and significant changes have taken place in daily life. These changes are increasing the welfare level of humankind. The work on material science has made a rapid progress especially in the field of electronics and properties such as semiconductor, photocatalytic activity make it possible to produce products with higher added value. According to these ideas and application fields, cadmium oxide (CdO) and zinc oxide (ZnO) are important semiconductor materials with remarkable optical band gap.

ZnO hexagonal crystal structure has exceptional properties and has a band width of 3.37eV especially at room temperature and that make it photocatalyst material (Kumar et al., 2014). Zinc oxide is used in many different applications such as solar cells, thin film transistors, photodiodes, chemical and gas sensors, optical and magnetic devices, and more (Aksoy & Ruzgar, 2015). There are many techniques to prepare zinc oxide such as spray pyrolysis (Lehraki et al., 2012), plasma enhanced chemical vapor deposition (B Arif, 2015), thermal evaporation (Hasim, Hamid, Shamsudin, & Jalar, 2009), magnetron sputtering (Jayaraman, Kuwabara, & Álvarez, 2016), and sol-gel method (Mujdat Caglar, Ilican, Caglar, & Yakuphanoglu, 2009). Recently, numerous reports have been reported on the

effects of dopant concentrations (Al, Cu, Ni, F, B, Ag, Na, In, and Li) on the structural, optical, and electrical properties have been reported(M Caglar & Yakuphanoglu, 2012; Xian et al., 2013).

Cadmium oxide is a material with n-type semiconductor and cubic crystal structure and is used in different optoelectronic products with direct 2.5 eV and indirect 1.98 eV. But the main issue for CdO thin films is low band gap for wider applications. By alloying with ZnO with CdO, the band gap of the composite can be red-shifted to blue, or even green light spectra range. In addition, the incorporation of Cd into ZnO is very useful for the fabrication of ZnO/$Zn_{1-x}Cd_xO$ heterojunction and super lattice, which is the key element in ZnO-based light emitters and detectors (Kim, Hong, & Uhm, 2007a; Mahmoud & Al-Ghamdi, 2010; Wang & Zhu, 2004). ZnO-CdO composites have been prepared such as nanowires (Shan, Liu, Zhang, Shen, & Hark, 2006), hollow micro-nanospheres(Li et al., 2008), nanorods (Kim, Hong, & Uhm, 2007b; Lv, Guo, Xu, & Chu, 2007) previously.

In this work, the composite materials were synthesized hydrothermally with semiconductor-based zinc oxide and cadmium oxide. The optical, crystal structure and electrical properties of the obtained products have been examined and interpreted.

2. Experimental

In our study, the Zinc nitrate hexahydrate$Zn(NO_3)_2.6H_2O$ (Carlo Erba, Analytical grade) and Cadmium nitrate tetrahydrate $Cd(NO_3)_2.4H_2O$ (Carlo Erba, Analytical grade) synthesized to obtain ZnO and CdO based composite material. ZnO and CdO materials are known as semiconductor materials and used in various applications (Margan & Haghighi, 2018). In the experiments, $Zn(NO_3)_2.6H_2O$ and $Cd(NO_3)_2.4H_2O$ were used as a precursor material in synthesis. $Zn(NO_3)_2.6H_2O$ 0.5M was dissolved in 8ml distilled water and 32ml ethylene glycol. Separately $Cd(NO_3)_2.4H_2O$ 0.8M was dissolved in 8ml distilled water and 32ml ethylene glycol. Both the zinc and cadmium solutions were mixed together in the volume ratios (20ml:60ml and 10ml:70ml) and so the total volume of solution was 80ml. The final solution was transferred to an autoclave and heated at 150 ˚C for 10 hours. The samples were prepared with following volume ratio as in Table 1.

Table 1. Volume ratios of the synthesised samples

Sample 1	$Cd(NO3)_2$ solution : ($Zn(NO_3)_2.6H_2O$) solution = 20ml : 60 ml
Sample 2	$Cd(NO3)_2$ solution : ($Zn(NO_3)_2.6H_2O$) solution = 10ml : 70 ml

After the autoclave, the obtained powder was filtered and washed several times with distilled water. Then the powder was dried at 60 ˚C for 24 hours. Finally, the powder samples were calcined at 450 ˚C.

In the analysis of the samples; the crystal phase of the prepared films was investigated using Rigaku-Ultima-IV X-ray diffractometer, utilizing Cu Kα radiation (λ = 0.15406 nm) operated at 40 kV, 30 mA. FTIR spectroscopyanalysis was done for compositional analysis (Thermo Scientific iS5). The optical spectra were measured by UV-VIS-NIR spectrophotometer (Shimadzu -3600PC). JEOL JSM-

7001F scanning electron microscopy (SEM) were employed to study the morphology of the films (Biroo, Canbay, Aziz, & Özkul, 2018; Biroo, Canbay, Ünlü, & Özkul, 2018).

3. Results and Discussions

3.1. Structural Analysis

Fig.1 shows the XRD pattern of ZnO-CdO nanocomposite powder through hydrothermal method. Two samples were prepared by mixing different volume ratio of $Zn(NO_3)_2$ and $Cd(NO_3)_2$ solutions. The prepared ZnO–CdO nanocomposite diffraction pattern shows both phases of hexagonal ZnO and cubic CdO. In the Fig.1. (a) for sample $Zn_{0.6}Cd_{0.2}$ the major three peaks correspond to CdO phase and matches very well JCPDS Card# 005-0640. CdO phase is dominant due to the presence of a sharp peak in the patterns. The diffraction pattern is shown in Fig.1 (a) for the $Zn_{0.6}Cd_{0.2}$sample. As clearly seen from Fig.1 (b) the diffraction pattern for $Zn_{0.7}Cd_{0.1}$ sample, the ZnO phase is dominant as compared to CdO because volume ratio of Zn precursor is increased further. It can be seen from Fig.1 that all the major peaks belong to zincite phase with hexagonal wurtzite crystal structure. The XRD diffraction pattern confirms the composition stoichiometry of the two samples prepared.

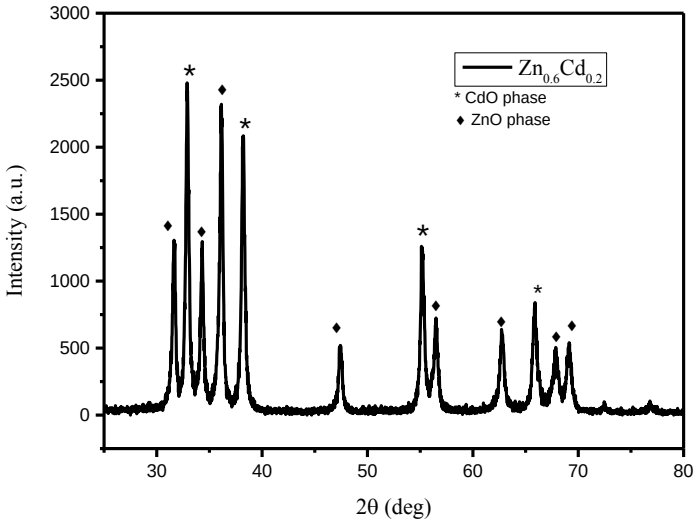

(a)

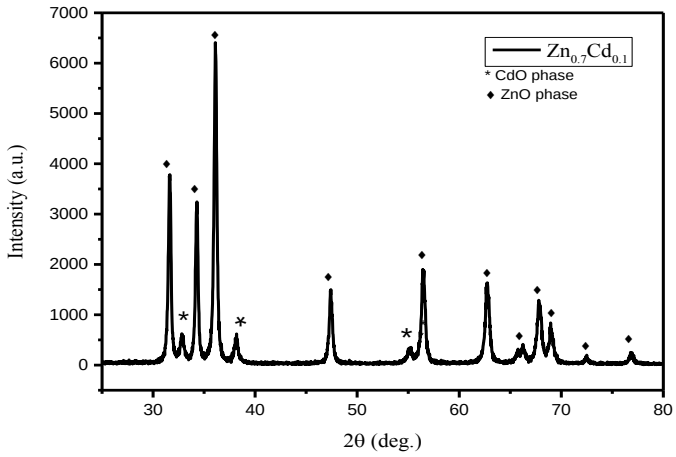

(b)

Figure 1. Diffraction patterns for (a) $Zn_{0.6}Cd_{0.2}$ (b) $Zn_{0.7}Cd_{0.1}$

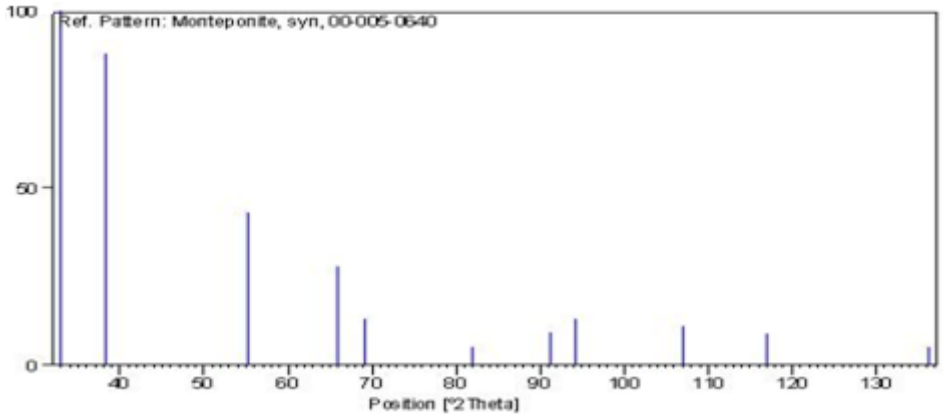

-a-

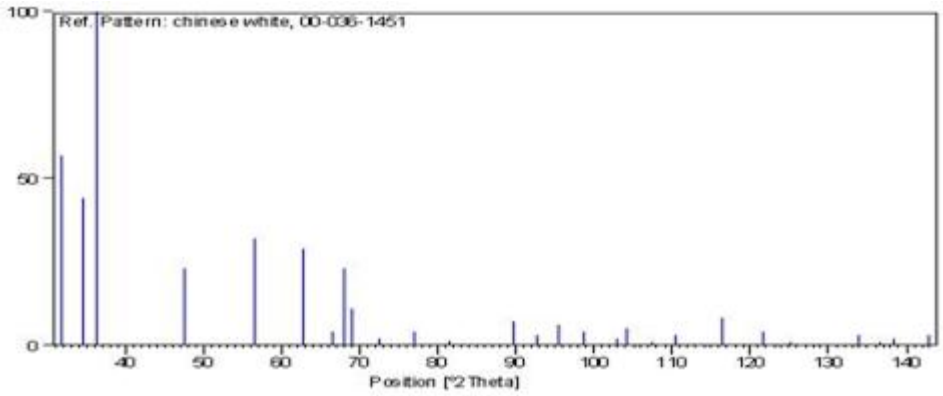

-b-

Figure 2. Reference pattern (a) JCPDS Card# 005-0640 for CdO (b) JCPDS Card # 036-1451 for ZnO.

The values of *d*-spacing, FWHM, and relative intensity corresponding to X-ray diffraction peaks for all two samples have been tabulated in Table 2. It is observed from the Table 2 that characteristic

peak (111) corresponding to CdO phase shifts from standard 33.002 towards lower angle. The ionic radii of Zn^{+2} (0.74) is smaller than Cd^{+2} (0.97). Considering the similar electronegativities of both Zn and Cd, therefore, Zn ions can easily substitute the Cd ions crystallographic positions. The replacement of Cd ions replaced by a smaller Zn ion as the Zn precursor volume is increased causes increase in d values and a corresponding decrease in 2θ towards lower angle. The similar results have been reported in (Jule et al., 2016). The value of lattice strain has been determined using the relation given below :

$$\varepsilon = \frac{\beta \cos\theta}{4} \tag{1}$$

where β is the full width (FWHM). The value of lattice strain obtained in this manner has been given Table 2. With the increase in the volume ratio of Zn precursor the lattice strain decreases. The value of crystallite size can be evaluated by Scherrer formula:

$$D = \frac{k\lambda}{\beta \cos\theta} \tag{2}$$

where k is the shape factor, λ is the wavelength of X-rays, and θ is the diffracting angle. The value of crystallite size determined in this manner has been given in Table 3. There is a slight increase in the value of crystallite size by increasing the volume of Zn precursor solution. Karthik et al (Karthik, Dhanuskodi, Gobinath, & Sivaramakrishnan, 2015) have also reported CdO-ZnO composite XRD diffraction pattern and calculated the microstrain values.

Table 2. Miller planes, 2θ, d-spacing, FWHM, percentage intensity for ZnO-CdO nanocomposite samples.

Sample	(hkl)	2θ(◦)	d(Å)	d(Å) Standard	FWHM (◦)	Intensity (%)
$Zn_{0.6}Cd_{0.2}$	111*	32.90	2.7201	2.7120	0.325	100
	101	36.12	2.4846	2.4759	0.368	92.9
	200*	38.24	2.3517	2.3490	0.366	84.6
	100	31.64	2.8255	2.8143	0.388	52.7
	002	34.30	2.6122	2.6033	0.304	51.5
	220*	55.22	1.6621	1.6610	0.424	50.3
$Zn_{0.7}Cd_{0.1}$	101	36.12	2.4847	2.4759	0.327	100
	100	31.62	2.8272	2.8143	0.320	59.7
	002	34.30	2.6123	2.6123	0.300	49.7

Table 3. 2θ, d-spacing, FWHM, Crystal size, Dislocation and Strain for ZnO-CdO nanocomposite samples.

Sample	2θ(◦)	d(A^o)	FWHM (◦)	Crystallite size (nm)	Dislocation δ (*10^{-4} nm)^2	Strain (*10^{-3})
$Zn_{0.6}Cd_{0.2}$	32.90	2.7201	0.325	25.49906	15.4	1.359
$Zn_{0.7}Cd_{0.1}$	36.12	2.4847	0.327	25.56505	15.3	1.356

3.2. FTIR Analysis

The FTIR spectra for ZnO-CdO nanocomposite has been recorded to study the various functional groups of nanocomposite as shown in Fig.3. The absorption band in the region of 3426 cm^{-1} corresponds to the O-H stretching vibrations of water present in the powder sample. The band in the region 1600-1500 cm^{-1} corresponds to the vibrations of a carboxyl group (CO). The characteristic wurtzite lattice vibrations (Zn-O) are corresponding with the broad band in the range of 400-600 cm^{-1}(Guan et al., 2012; Jule et al., 2016; Rana, Chand, & Gathania, 2015). It can be clearly seen that the peaks around 600-500 cm^{-1}in sample $Zn_{0.6}Cd_{0.2}$ and $Zn_{0.7}Cd_{0.1}$ as Zn volumetric ratio was increased in the composite. The well-known stretching mode of CdO was observed at 1420 cm^{-1} (Jule et al., 2016).

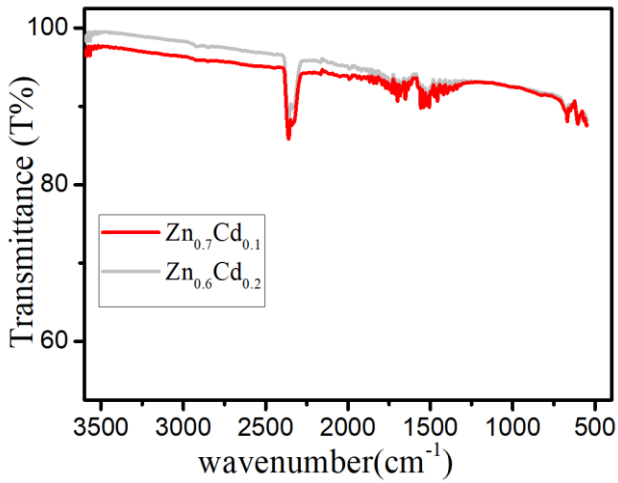

Figure 3. FTIR spectra for ZnO-CdO composite for$Zn_{0.6}Cd_{0.2}$and $Zn_{0.7}Cd_{0.1}$ samples.

3.3. Morphological Analysis

The surface morphology of ZnO-CdO nanocomposite was studied using FESEM at various magnifications and shown in Fig. (4-5). The morphology consists of spherical, non-spherical and partly cylindrical structures. In the first sample $Zn_{0.6}Cd_{0.2}$ (Fig.4) at x30000 magnification, the connectivity between partially cylindrical structures is found which might be developed due to sintering necks between spherical particles. When further increasing the Zn content can be seen in the SEM micrographs of second sample $Zn_{0.7}Cd_{0.1}$ (Fig.5.) the morphology of the composite changes. The compositional analysis of ZnO-CdO composite was confirmed by EDX (Table 4). The EDX spectrum for each sample

is shown below the SEM micrographs. The spectra clearly show the presence of Zn, O, and Cd elements along with peak of Au. The Au peak is due to the coating of Au film on the powder samples before FESEM/EDX.

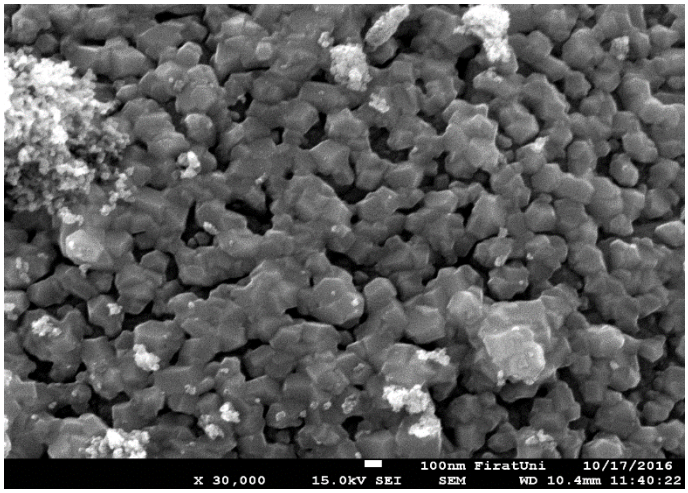

(a)

Figure 4. SEM micrograph for $Zn_{0.6}Cd_{0.2}$ at **(a)** 30000x magnification.

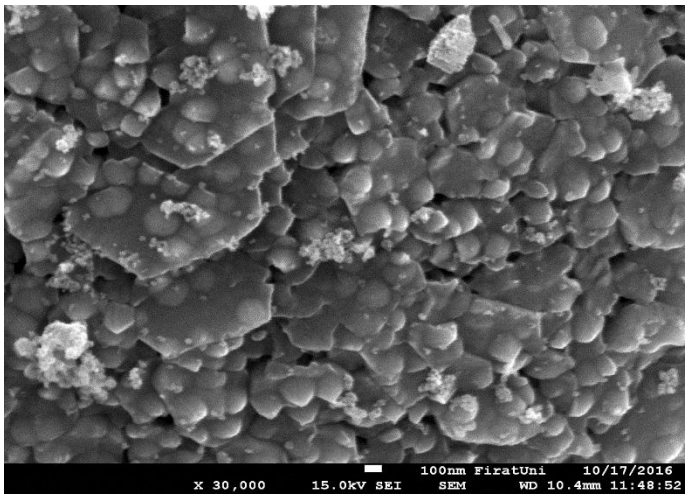

(a)

Figure 5. SEM micrograph for $Zn_{0.7}Cd_{0.1}$ at **(a).** 30000x magnification.

Table 4.EDX analysis of samples.

	Elements	Weight%	Atomic%
$Zn_{0.7}Cd_{0.1}$ sample	O	14.53	41.75
	Zn	79.15	55.66
	Cd	6.32	2.58
$Zn_{0.6}Cd_{0.2}$ sample	O	16.11	54.32
	Zn	15.69	12.95
	Cd	68.20	32.73

3.4. optical analysis

The spectral distribution of reflectance R(λ) at the normal incident for all the samples is shown in Fig. 6. The light penetrates inside the sample and undergoes a combination of scattering and absorption inside the sample. Some of the radiation is reflected back towards the surface. This reflected radiation contains useful information due to a higher order of interaction. The reflected radiation is called Kubelka-Munk (KM) reflectance and is defined by a function. The KM function F(R), can be used to approximate the optical absorbance of the sample from is reflectance and is given by (Martellucci, Chester, & Mignani, 2002).

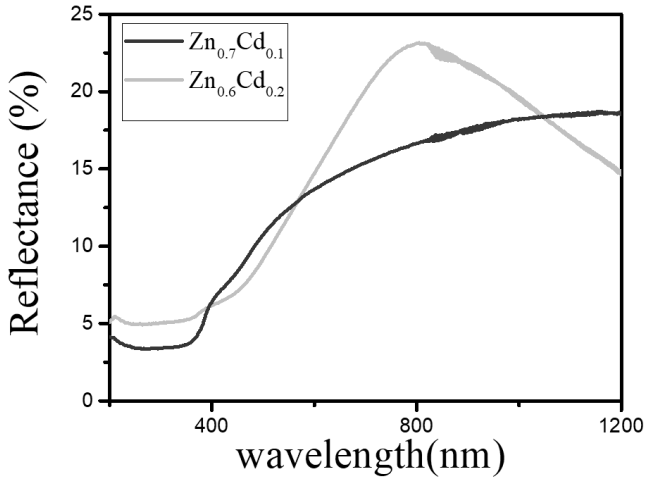

Figure 6. Reflectance spectra for ZnO-CdO composites with various composition.

$$F(\mathrm{R}) = \frac{(1-R)^2}{2R} \tag{3}$$

So by replacing the absorption coefficient α in the Tauc's relation can be get as;

$$(F(R)hv)^2 \propto (hv - E_g) \tag{4}$$

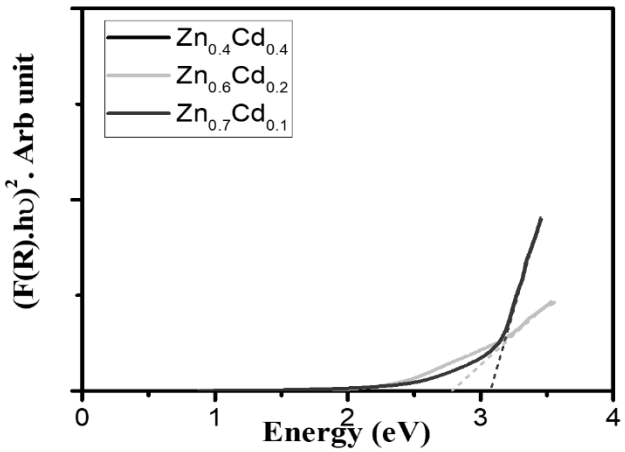

Figure 7. Bandgap for ZnO-CdO composites with various composition.

For the direct band gap, the plot between $(F(R).h\nu)^2$ and photon energy ($h\nu$) has been shown in Fig.7. The band gap value can be determined by extrapolating the graph of the linear region of the plots to energy axis at $(F(R).h\nu)^2 = 0$ (Bilal Arif et al., 2015). The band gap value for sample $Zn_{0.6}Cd_{0.2}$ bandgap energy is found to be 2.78 eV. The bandgap value for $Zn_{0.7}Cd_{0.1}$ increases to 3.06 eV with further increase of volume concentration of Zn. The blue shift has been observed on increase in Zn precursor solution volume. The bandgap value for pure ZnO and CdO are 3.3 ev and 2.5 ev(Chandiramouli & Jeyaprakash, 2013). The increase in Zn content causes the lower states in conduction band to be filled and hence leading the blue shift in bandgap energies. The similar trends in bandgap energies have been reported by Jule at al and R. Saravanan et al (Jule et al., 2016; Saravanan et al., 2015).

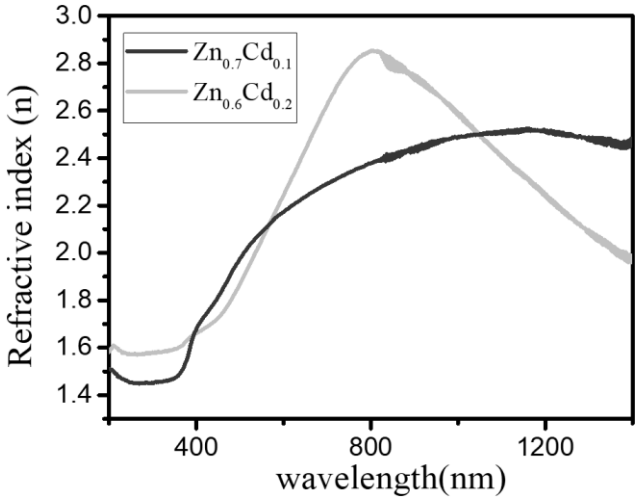

Figure 8. Refractive index for ZnO-CdO composites with various composition.

The study of dispersion is crucial for the application of any material in the field of integrated optical devices and device design for optical communication and spectral dispersion. The refractive index of the film was determined by the following relation (El-Nahass, Farag, & Atta, 2009).

$$n = \left[\frac{1+R}{1-R}\right] + \sqrt{\frac{4R}{(1-R)^2} - K^2} \qquad (5)$$

where $K = \alpha\lambda/4\pi$ is the extinction coefficient. The variation in refractive index has been shown in Fig. 8.

3.5. Thermal Analysis

Thermal measurements such as TG/DTA were made to determine the weight loss of the samples by the effect of heating, quality of the product and phase transitions from room temperature to high temperature and also the phase stability. The measurements were made with a heating rate of 10 ˚C/min.

from room temperature to 925 ˚C. The TG/DTA curves of the samples are given in Fig.9 a and Fig.9 b. The weight loss of sample $Zn_{0.6}Cd_{0.2}$ is 4.71% and for the sample $Zn_{0.7}Cd_{0.1}$ is 2.57%. For both samples, a small endothermic peak was observed in DTA analysis and this peak belongs to residues of the samples.

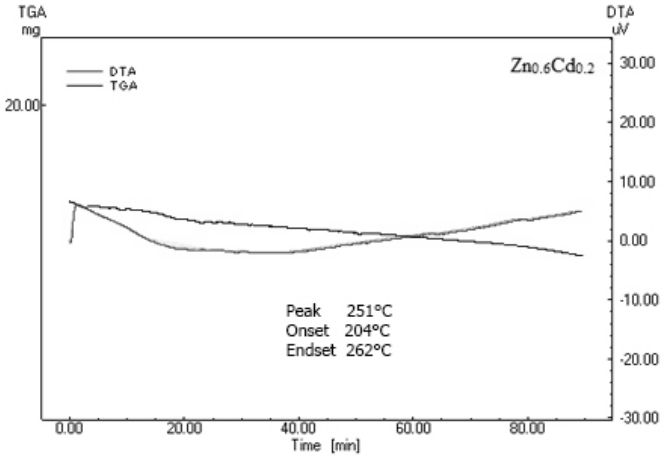

(a)

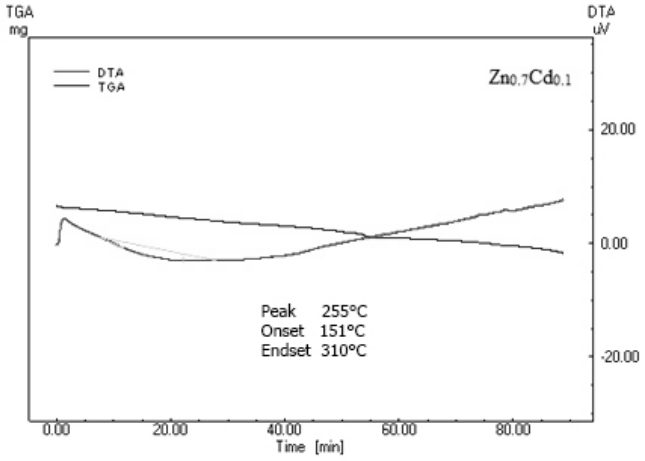

(b)

Figure 9.TG-TDA analysis of a) $Zn_{0.6}Cd_{0.2}$ sample and b)$Zn_{0.7}Cd_{0.1}$ sample.

3.6. Electrical Conductivity

In order to investigate the electrical properties of the samples, the dc conductivity of the samples was measured using two probe method. The I-V graph for the two samples has been shown in Figure 10. The electrical conductivity of the samples was found as $1.3x10^{-3}$ and $4.4x10^{-8}$ S/cm, respectively. It can be clearly see from the graphs below that the conductivity is decreased with the increase in Zn content. K. Ocakoglu et. al. (Ocakoglu et al., 2015) has reported the electrical conductivity of ZnO nanorods at room temperature is $6.7x10^{-8}$ S/cm. The reported value is very close to the sample $Zn_{0.7}Cd_{0.1}$ conductivity value. In the ZnO-CdO composite, the ZnO have hexagonal wurtzite structure and CdO

have a cubic crystal structure that causes the phase segregation. Thus, this phase segregation, crystal strain, grain boundary barrier effects may enhance the electron scattering and cause the deterioration in conductivity.

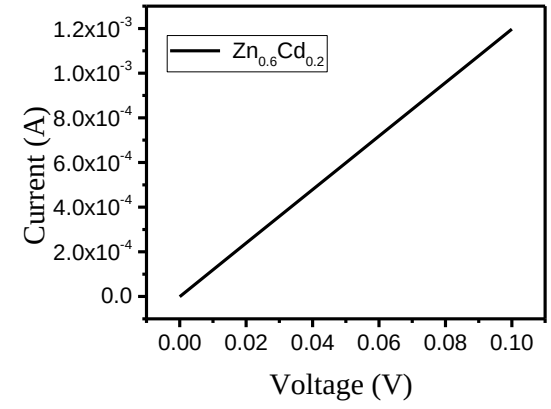

(a)

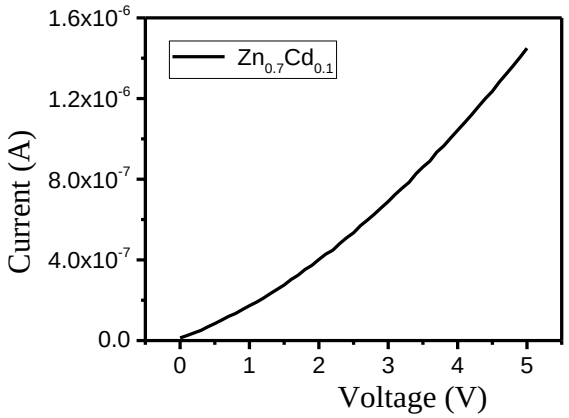

(b)

Figure 10. DC Conductivity of ZnO-CdO composites for **(a)** $Zn_{0.6}Cd_{0.2}$ **(b)** $Zn_{0.7}Cd_{0.1}$

4. Conclusions

The ZnO-CdO composite was synthesized by using the hydrothermal technique. The structural analysis was done using the X-ray diffraction. The morphological properties were investigated by using FESEM and in these images some spherical and non-spherical particles can be seen. The bandgap values of the two samples were 2.78 and 3.06 eV, respectively which are in agreement with previously reported values. The thermal analysis graphs confirm the formation of stability in composites. The dc conductivity of the pallets was measured and value of conductivity decreases with increase in Zn volume concentration.

Acknowledgement

Data in this paper was previously published as a conference paper in "International Engineering and Technology Symposium (IEST'18), May 2018".

5. References

[1]. Aksoy, S, & Ruzgar, S. (2015). Effect of Nitrogen on optical properties of ZnO film deposited by sol gel method. *J Mater Electron Dev, 1*, 33-37.

[2]. Arif, B. (2015). Determination of optical constants of ZnO growth by PECVD Method. *J Mater Electron Dev, 1*, 28-32.

[3]. Arif, Bilal, El-Nasser, HM, Dere, A, Al-Ghamdi, Ahmed A, Bin-Omran, S, El-Tantawy, Farid, & Yakuphanoglu, F. (2015). Optical properties of Zn1− xAlxO: NiO transparent metal oxide composite thin films prepared by sol–gel method. *Journal of Sol-Gel Science and Technology, 76*(2), 378-385.

[4]. Biroo, Safiye Jameel, Canbay, Canan AKSU, Aziz, Sivar, & Özkul, İskender. (2018). *Structural properties of CdO-ZnO Semiconductor Composite*. Paper presented at the 1st International Engineering and Technology Symposium, Batman.

[5]. Biroo, Safiye Jameel, Canbay, Canan AKSU, Ünlü, Nihan, & Özkul, İskender. (2018). *Optical properties of ZnO-3CdO Synthesized by Hydrothermal Method*. Paper presented at the 1st International Engineering and Technology Symposium, Batman.

[6]. Caglar, M, & Yakuphanoglu, F. (2012). Structural and optical properties of copper doped ZnO films derived by sol–gel. *Applied Surface Science, 258*(7), 3039-3044.

[7]. Caglar, Mujdat, Ilican, Saliha, Caglar, Yasemin, & Yakuphanoglu, Fahrettin. (2009). Electrical conductivity and optical properties of ZnO nanostructured thin film. *Applied surface science, 255*(8), 4491-4496.

[8]. Chandiramouli, R, & Jeyaprakash, BG. (2013). Review of CdO thin films. *Solid State Sciences, 16*, 102-110.

[9]. El-Nahass, MM, Farag, AAM, & Atta, AA. (2009). Influence of heat treatment and gamma-rays irradiation on the structural and optical characterizations of nano-crystalline cobalt phthalocyanine thin films. *Synthetic Metals, 159*(7), 589-594.

[10]. Guan, Rongfa, Kang, Tianshu, Lu, Fei, Zhang, Zhiguo, Shen, Haitao, & Liu, Mingqi. (2012). Cytotoxicity, oxidative stress, and genotoxicity in human hepatocyte and embryonic kidney cells exposed to ZnO nanoparticles. *Nanoscale research letters, 7*(1), 602.

[11]. Hasim, Siti Nuurul Fatimah, Hamid, Muhammad Azmi Abdul, Shamsudin, Roslinda, & Jalar, Azman. (2009). Synthesis and characterization of ZnO thin films by thermal evaporation. *Journal of Physics and Chemistry of Solids, 70*(12), 1501-1504.

[12]. Jayaraman, Vinoth Kumar, Kuwabara, Yasuhiro Matsumoto, & Álvarez, Arturo Maldonado. (2016). Importance of substrate rotation speed on the growth of homogeneous ZnO thin films by reactive sputtering. *Materials Letters, 169*, 1-4.

[13]. Jule, Leta T, Dejene, Francis B, Ali, Abdub G, Roro, Kittessa T, Hegazy, Aiat, Allam, Nageh K, & El Shenawy, Essam. (2016). Wide visible emission and narrowing band gap in Cd-doped ZnO nanopowders synthesized via sol-gel route. *Journal of Alloys and Compounds, 687*, 920-926.

[14]. Karthik, K, Dhanuskodi, S, Gobinath, C, & Sivaramakrishnan, S. (2015). Microwave-assisted synthesis of CdO–ZnO nanocomposite and its antibacterial activity against human pathogens. *Spectrochimica Acta Part A: Molecular and Biomolecular Spectroscopy, 139*, 7-12.

[15]. Kim, Jong Hun, Hong, Yong Cheol, & Uhm, Han Sup. (2007a). Binary oxide material made from a mixture of Zn and Cd in a microwave plasma. *Chemical physics letters, 443*(1), 122-126.

[16]. Kim, Jong Hun, Hong, Yong Cheol, & Uhm, Han Sup. (2007b). Synthesis of oxide nanoparticles via microwave plasma decomposition of initial materials. *Surface and Coatings Technology, 201*(9), 5114-5120.

[17]. Kumar, P Senthil, Selvakumar, M, Bhagabati, Purabi, Bharathi, B, Karuthapandian, S, & Balakumar, S. (2014). CdO/ZnO nanohybrids: facile synthesis and morphologically enhanced photocatalytic performance. *Rsc Advances, 4*(62), 32977-32986.

[18]. Lehraki, N, Aida, MS, Abed, S, Attaf, N, Attaf, A, & Poulain, Marcel. (2012). ZnO thin films deposition by spray pyrolysis: influence of precursor solution properties. *Current Applied Physics*, *12*(5), 1283-1287.

[19]. Li, Guangming, Wang, Xinchang, Wang, Yinghua, Shi, Xinwei, Yao, Ning, & Zhang, Binglin. (2008). Synthesis and field emission properties of ZnCdO hollow micro–nano spheres. *Physica E: Low-dimensional Systems and Nanostructures*, *40*(8), 2649-2653.

[20]. Lv, Yuzhen, Guo, Lin, Xu, Hubin, & Chu, Xiangfeng. (2007). Gas-sensing properties of well-crystalline ZnO nanorods grown by a simple route. *Physica E: Low-dimensional Systems and Nanostructures*, *36*(1), 102-105.

[21]. Mahmoud, Waleed E, & Al-Ghamdi, AA. (2010). Synthesis of CdZnO thin film as a potential candidate for optical switches. *Optics & Laser Technology*, *42*(7), 1134-1138.

[22]. Margan, Payam, & Haghighi, Mohammad. (2018). Sono-coprecipitation synthesis and physicochemical characterization of CdO-ZnO nanophotocatalyst for removal of acid orange 7 from wastewater. *Ultrasonics Sonochemistry*, *40*, 323-332.

[23]. Martellucci, Sergio, Chester, Arthur N, & Mignani, Anna Grazia. (2002). Optical Sensors and Microsystems. *New York, Boston, London*.

[24]. Ocakoglu, K, Mansour, Sh A, Yildirimcan, S, Al-Ghamdi, Ahmed A, El-Tantawy, F, & Yakuphanoglu, F. (2015). Microwave-assisted hydrothermal synthesis and characterization of ZnO nanorods. *Spectrochimica Acta Part A: Molecular and Biomolecular Spectroscopy*, *148*, 362-368.

[25]. Rana, N, Chand, Subhash, & Gathania, Arvind K. (2015). Tailoring the structural and optical properties of ZnO by doping with Cd. *Ceramics International*, *41*(9), 12032-12037.

[26]. Saravanan, R, Gracia, F, Khan, Mohammad Mansoob, Poornima, V, Gupta, Vinod Kumar, Narayanan, V, & Stephen, A. (2015). ZnO/CdO nanocomposites for textile effluent degradation and electrochemical detection. *Journal of Molecular Liquids*, *209*, 374-380.

[27]. Shan, CX, Liu, Z, Zhang, ZZ, Shen, DZ, & Hark, SK. (2006). A simple route to porous ZnO and ZnCdO nanowires. *The Journal of Physical Chemistry B*, *110*(23), 11176-11179.

[28]. Wang, Wei-Wei, & Zhu, Ying-Jie. (2004). Shape-controlled synthesis of zinc oxide by microwave heating using an imidazolium salt. *Inorganic Chemistry Communications*, *7*(9), 1003-1005.

[29]. Xian, Fenglin, Miao, Kaibo, Bai, Xuecheng, Ji, Yun, Chen, Feier, & Li, Xiangyin. (2013). Characteraction of Ag-doped ZnO thin film synthesized by sol–gel method and its using in thin film solar cells. *Optik-International Journal for Light and Electron Optics*, *124*(21), 4876-4879.